

# Spreading with immunization in high dimensions

Stephan M Dammer<sup>1</sup> and Haye Hinrichsen<sup>2</sup>

<sup>1</sup>Institut für Physik, Universität Duisburg-Essen, D-47048 Duisburg, Germany

<sup>2</sup>Fakultät für Physik und Astronomie, Universität Würzburg, D-97074 Würzburg, Germany

**Abstract.** We investigate a model of epidemic spreading with partial immunization which is controlled by two probabilities, namely, for first infections,  $p_0$ , and reinfections,  $p$ . When the two probabilities are equal, the model reduces to directed percolation, while for perfect immunization one obtains the general epidemic process belonging to the universality class of dynamical percolation. We focus on the critical behavior in the vicinity of the directed percolation point, especially in high dimensions  $d > 2$ . It is argued that the clusters of immune sites are compact for  $d \leq 4$ . This observation implies that a recently introduced scaling argument, suggesting a stretched exponential decay of the survival probability for  $p = p_c$ ,  $p_0 \ll p_c$  in one spatial dimension, where  $p_c$  denotes the critical threshold for directed percolation, should apply in any dimension  $d \leq 3$  and maybe for  $d = 4$  as well. Moreover, we show that the phase transition line, connecting the critical points of directed percolation and of dynamical percolation, terminates in the critical point of directed percolation with vanishing slope for  $d < 4$  and with finite slope for  $d \geq 4$ . Furthermore, an exponent is identified for the temporal correlation length for the case of  $p = p_c$  and  $p_0 = p_c - \epsilon$ ,  $\epsilon \ll 1$ , which is different from the exponent  $\nu_{\parallel}$  of directed percolation. We also improve numerical estimates of several critical parameters and exponents, especially for dynamical percolation in  $d = 4, 5$ .

PACS numbers: 05.50.+q, 05.70.Ln, 64.60.Ht

## 1. Introduction

The study of stochastic models that describe the spreading of a nonconserved agent is currently a very active field of research in nonequilibrium statistical physics [1, 2, 3]. Fundamental interest stems from the fact that these models exhibit continuous nonequilibrium phase transitions from a fluctuating active phase into one or several absorbing states. Moreover, such models are motivated by a variety of possible applications [4] such as epidemic spreading [5, 6], catalytic reactions [7], or flowing sand [8, 9].

Usually models for epidemic spreading are defined on a lattice whose sites can be either occupied (active, infected) or empty (inactive, healthy). The dynamic rules involve two competing processes, namely, spreading of activity to neighboring sites (infection) and spontaneous decay (recovery). Depending on the relative frequency of infection and recovery the process either has a finite probability to survive in an infinite system or it will eventually die out. Since the spreading agent is not allowed to be created spontaneously, once the empty lattice is reached, the process is trapped in a so-called *absorbing state* from which it cannot escape. Usually the transition between infinite spreading and recovery is a critical phenomenon characterized by large-scale fluctuations associated with certain universality classes. Therefore, the classification of all possible types of phase transitions into absorbing states is presently one of the major goals of nonequilibrium statistical physics.

The most prominent universality class of phase transitions into an absorbing state is that of directed percolation (DP) [10], as described by Reggeon field theory [11, 12, 13]. Models in this class describe short-range spreading of a non-conserved agent in a medium without temporal memory effects. Additionally, it is assumed that the rates for spreading and recovery are constant in space and time (no quenched randomness).

If the medium has a memory such that each site can be infected only once, the transition does no longer belong to the DP class, instead one obtains the so-called “general epidemic process” (GEP) [5, 14]. In the language of epidemic processes this type of memory accounts for *perfect* immunization. In contrast to DP, where sites can be reinfected without restriction, a general epidemic process can only spread in those parts of the system which have not been infected before. Nevertheless, in spatial dimensions  $d \geq 2$ , infinite spreading from a single infected site in a non-immune environment is still possible, provided that the susceptibility to primary infections is sufficiently large. In this case activity propagates as a front, leaving a cluster of immune sites behind. The transition between survival and extinction of the spreading agent is then described by a different type of critical behavior, belonging to the universality class of dynamical percolation (DyP) [15]. In fact, the resulting cluster of immune sites has the same (or even identical) structure as an isotropic percolation cluster. For this reason DyP can be used as a dynamical procedure to generate isotropic percolation clusters.

As an immediate generalization one may consider an epidemic process in which

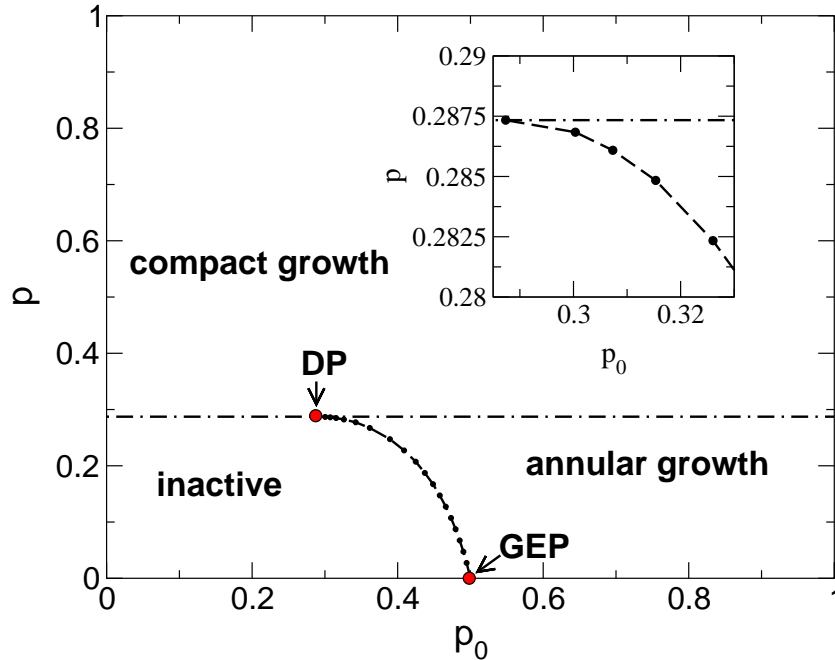


**Figure 1.** Phase diagram of the epidemic process with finite immunization on a square lattice in 2+1 dimensions.  $p_0$  denotes the primary infection probability and  $p$  the refection probability. The inset shows the vicinity of the DP point.

the strength of immunization can be varied [16]. For example, the initial susceptibility to infections  $p_0$  may be locally set to a different value  $p$  when the first infection is encountered. In the following we shall denote this process as epidemic process with finite immunization which we abbreviate for convenience as EPFI. The phase diagram of the EPFI in two spatial dimensions was studied in [17]. As shown in Fig. 1, it comprises three different phases, including the GEP ( $p = 0$ ) and DP ( $p = p_0$ ) as special cases.

The horizontal phase transition line in Fig. 1 can be explained as follows. Obviously, when starting from a fully occupied lattice, all sites become immediately immune so that the infection rate is everywhere equal to  $p$ . Trivially, the dynamics is then precisely that of a DP process controlled by  $p$ . This gives rise to a DP transition at  $p = p_c$ , independent of  $p_0$ , where  $p_c$  denotes the critical value of an ordinary DP process. However, starting with a localized infected seed in a non-immune environment, the situation is more subtle, though the horizontal line still exists. For example, slightly above the critical line, i.e. for  $p = p_c + \epsilon$  with  $\epsilon \ll 1$ , the interior of a surviving cluster is essentially dominated by an ordinary supercritical DP process. Since such a DP process is characterized on large scales by a finite density of active sites, there will be a finite chance for the process to survive in the limit  $t \rightarrow \infty$  [17].

The situation below the horizontal line ( $p < p_c$ ) is different. In at least two or more dimensions this part of the phase diagram displays *two* distinct phases, namely, an absorbing phase, where the process stops after some time, and a phase of annular growth,

where an expanding front of high activity survives with finite probability. Performing a field-theoretic renormalization group study close to the upper critical dimension of DyP,  $d_c^{\text{DyP}} = 6$ , and computing the corresponding critical exponents, Janssen showed that the critical behavior along the line connecting the GEP and the DP point in Fig. 1 is that of DyP [18]. In this sense immunization is a relevant perturbation, driving the system away from the DP point in Fig. 1 towards GEP. (We note that in the case of several competing infections with immunization, one observes a crossover back to DP [6]. Another four-state generalization leads to an interesting tricritical phenomenon belonging to a different universality class [19]).

More recently epidemic spreading with immunization appeared in a different context. Studying systems with infinitely many absorbing states such as the non-diffusive pair contact process [20, 21], Muñoz *et al* conjectured that these models are described by the same type of field theory as the EPFI [22, 23]. Roughly speaking, the frozen absorbing configurations generated by the process provide a local memory of activity in the past which effectively acts in the same way as immunization (or weakening). Meanwhile this conjecture is widely accepted, although some questions concerning the upper critical dimension are still debated [24, 25].

While the mentioned field-theoretic results explain the transition line between the GEP and the DP point close to  $d_c^{\text{DyP}} = 6$ , the critical properties along the horizontal line and in the vicinity of the DP point are less well understood. Simulating the Langevin equation of the EPFI at critical reinfection rate (corresponding to the horizontal line in Fig. 1) in 1+1 dimensions starting with a localized seed, López and Muñoz initially expected continuously varying exponents [26], but refined simulations and approximations suggest that there is no power-law scaling. Instead, the activity was found to vary as a stretched exponential in 1+1 dimensions [17, 27].

In this paper we study the epidemic process with finite immunization, focussing on the influence of immunization in the vicinity of the DP point, especially in higher dimensions  $d > 2$ . In Sec. 2 we describe Monte Carlo simulations that are applied in the following sections to obtain numerical results. In Sec. 3 we summarize the most important phenomenological features of the process. In particular, we argue that the clusters of immune sites at the DP point are *compact* for  $d \leq 3$  and *asymptotically compact* for  $d = 4$  (see below). Consequently, a recently introduced scaling argument that suggested a stretched exponential decay on the horizontal line for  $p_0 \ll p_c$  in  $d = 1$  [27] should apply in any dimension  $d \leq 3$  and maybe for  $d = 4$  as well, since it is based essentially on the compactness of the cluster of immune sites. This means that we expect a stretched exponential decay instead of power-law behavior not only in one but also in two, three and perhaps four spatial dimensions. Moreover, for  $d < 4$ , primary infections and reinfections scale differently whereas they show the same scaling behavior for  $d \geq 4$ . As a result, we find that the phase transition line connecting the GEP and the DP point should terminate in the DP point with a *finite* slope for  $d \geq 4$  (in contrast to a vanishing slope for  $d < 4$ , as can be seen in Fig. 1). In Sec. 4 we discuss the Langevin

equation for EPFI in order to describe how the properties of the process change between the upper critical dimension of DP,  $d_c^{\text{DP}} = 4$ , and DyP,  $d_c^{\text{DyP}} = 6$ . Numerically determined phase diagrams for  $d > 2$  are presented in Sec. 5, which support the predictions of Sec. 3. Though we expect the behavior along the horizontal phase transition line to be non-universal (at least for  $d \leq 4$ ), it is nevertheless possible to identify an exponent  $\mu$  for the temporal correlation length in the case of  $p = p_c$  and  $p_0 = p_c - \epsilon$  for  $\epsilon \ll 1$ . As discussed in Sec. 6, this exponent differs from the critical exponent for the temporal correlation length of DP. The main results are summarized in Sec. 7. A heuristic argument for the value of  $\mu$  that is in accordance with the numerical data is presented in Appendix A. Numerical estimates for critical parameters and critical exponents for DP and DyP are given in Appendix B and Appendix C, respectively.

## 2. Monte Carlo simulations

We perform Monte Carlo (MC) simulations of the epidemic process with finite immunization on a simple  $d$ -dimensional cubic lattice using the model of Ref. [17] generalized to arbitrary dimensions. The process is defined such that it reduces to directed *bond* percolation at the DP point and to dynamical *bond* percolation at the GEP point. In particular, an active lattice site  $i$  at time  $t$  may activate each of its  $d$  nearest neighbors, denoted as  $j$ , at the next discrete time step  $t + 1$ . If neighbor  $j$  has never been active before, activity is transmitted from site  $i$  to site  $j$  with the primary infection probability  $p_0$ . Contrarily, if site  $j$  has been active at least once in the past the infection probability is given by  $p$ , called reinfection probability. Each site stays active only for one time step.

The process is initialized with an active seed at the origin at time  $t = 0$  in a non-immune environment. Each run is stopped either when the process dies out or when it reaches a preset maximum time. We average over many runs with different realizations of randomness. The lattice is always chosen large enough so that the process never reaches its boundary. Hence, finite size effects are eliminated. As usual in such 'seed simulations' we measure the survival probability  $P_s(t)$  that the process survives at least up to time  $t$ , the number of active sites averaged over all runs  $N(t)$ , and the mean square spreading from the origin  $R^2(t)$  averaged over surviving runs. At criticality these quantities obey power-laws [28, 29] according to

$$P_s(t) \sim t^{-\delta} \quad , \quad N(t) \sim t^\theta \quad , \quad R^2(t) \sim t^{2/z} \quad . \quad (1)$$

This behavior is observed for critical DP as well as for critical DyP. Of course, the exponents in Eq. (1) are generally different in both cases. In addition, we also measure the number of primary infections  $n_p$  (see below).

From a technical point of view, our simulations for  $d \geq 3$  are based on the routine presented in [30]. Lattice sites are labeled by 64-bit-long integers. We do not initialize storage for a whole  $L^d$  lattice since for high dimensions it is only possible to simulate

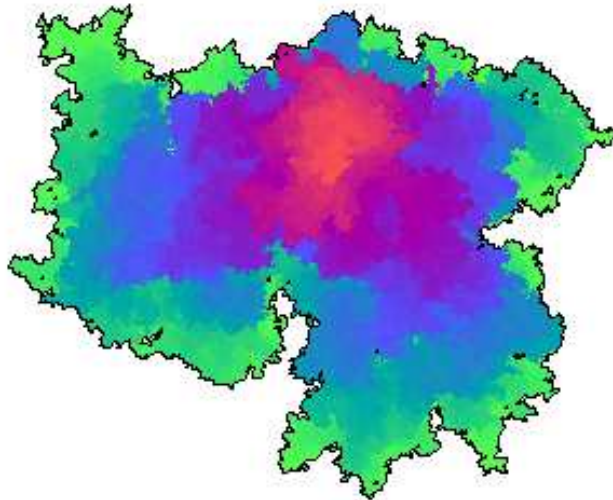


**Figure 2.** Typical cluster of immune sites generated by the EPFI in 2+1 dimensions at the DP point after 2048 updates. The colors represent linearly the time at which the sites were visited for the first time. The black line marks the final boundary of the cluster.

small lateral lattice sizes  $L$  with this method. Instead we use lists to store the individual positions of active and immune sites. To perform an update from  $t$  to  $t+1$  we go through all active sites at time  $t$  and activate their neighbors at time  $t+1$  with probability  $p_0$  or  $p$ , respectively. The activated sites are stored in a list while the formerly active sites recover. In the case of a first infection, the site is added to the list of immune sites. In order to efficiently check whether a site is immune or not, and whether it has already been activated during the actual update step, we use a hashing algorithm as described in [30]. Contrarily, the simulations for  $d = 1, 2$  are carried out in the usual way where one initializes storage for a whole lattice. However, in this case we apply bit-coding, i.e., a single 64-bit-long integer stores the states of 64 lattice sites (active/inactive or immune/non-immune).

### 3. Phenomenological properties

Let us first consider the phenomenological properties of the process near the DP point, where the effect of immunization is small. Since the DP point itself is a critical DP process, the question arises how the upper critical dimension of DP influences the generated cluster of immune sites. As a conjecture we propose that the generated cluster of immune sites at the DP point is *compact* in  $d < 4$  dimensions (in the sense that its fractal dimension is  $d$ ), while in higher dimensions  $d > 4$  it is not. At the DP point  $p = p_0 = p_c$ , the influence of immunization vanishes so that the cluster of immune sites is merely given by the sites visited in the past by a critical DP process. In other words, when projecting the past activity of a critical DP cluster onto space (looking

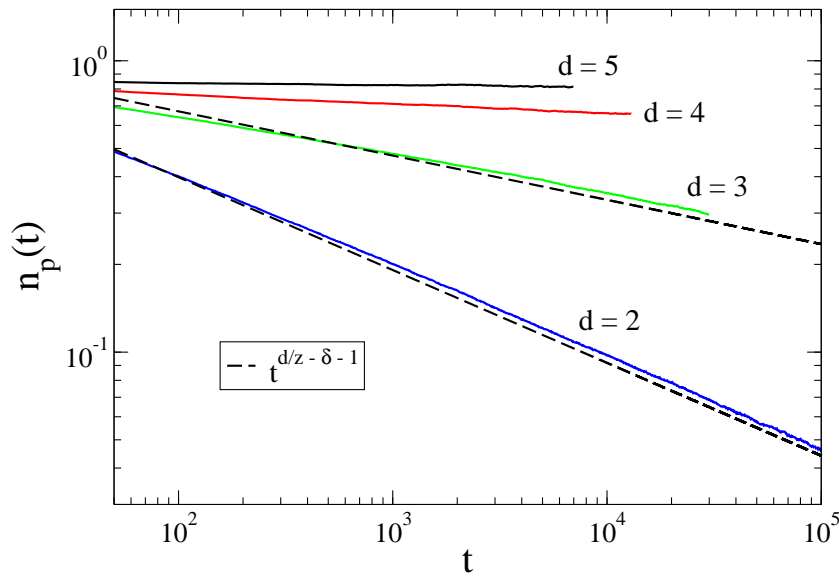


**Figure 3.** Double logarithmic plot of the number of primary infections versus time at the DP point for various dimensions. For comparison the power-law behavior predicted by Eq. (3) is shown by the dashed lines for  $d = 2, 3$ . For  $d = 4$  the mean-field prediction of Eq. (3) is  $n_p(t) = \text{const}$ .

through a critical DP cluster along the temporal axis) we expect its appearance to be compact in  $d < 4$ . Obviously, in  $d = 1$  the cluster of visited sites is compact by definition so that the conjecture is correct. In dimensions  $d = 2, 3$  the statement is non-trivial. In fact, plotting the projection of a typical cluster in  $d = 2$  dimensions one obtains a compact object, as shown in Fig. 2.

The above conjecture can be supported numerically as follows. Assuming compactness, the number of immune sites in a surviving run should grow linearly with the volume  $\xi_{\perp}^d$ , where  $\xi_{\perp} \sim t^{1/z}$  is the spatial correlation length and  $z = \nu_{\parallel}/\nu_{\perp}$  is the dynamical exponent of DP (see, e.g., [2]). Averaging over all runs, the volume has to be multiplied with the survival probability  $P_s(t) \sim t^{-\delta}$ , where  $\delta = \beta/\nu_{\parallel}$ , hence the average number of immune sites  $I(t)$  increases as

$$I(t) \sim t^{d/z - \delta}. \quad (2)$$

This implies that the number of *primary* infections  $n_p$  scales as the derivative of  $I(t)$ , i.e.,

$$n_p(t) \sim t^{d/z - \delta - 1}. \quad (3)$$

As shown in Fig. 3 by numerical simulations, in  $d = 2, 3$  this quantity scales indeed according to Eq. (3), supporting that the generated clusters of immune sites are compact.

For  $d = 4$  the data still exhibits a slight curvature which is presumably due to logarithmic corrections [31, 32] that affect the mean-field behavior ( $n_p = \text{const}$ ) at the

upper critical dimension of DP,  $d_c^{\text{DP}} = 4$ . As usual, also for  $d > d_c^{\text{DP}}$  we observe mean-field behavior and thus we expect the resulting cluster of immune sites to be non-compact.

It is also possible to support the conjecture by a scaling argument. Obviously  $I(t)$  cannot be larger than the integrated past activity  $\int_0^t dt' N(t') \sim t^{1+\theta}$  [28], leading to the inequality

$$d/z - \delta \leq \theta + 1. \quad (4)$$

as a necessary condition for compactness. In  $d < 4$  dimensions the initial-slip exponent  $\theta$  is given by the hyperscaling relation [28, 33]

$$\theta = d/z - 2\delta \quad (5)$$

so that the inequality reduces to  $\delta \leq 1$ , which is indeed satisfied in  $d < 4$  (see Tab. B1). At the upper critical dimension of DP,  $d_c^{\text{DP}} = 4$ , taking the mean-field exponents  $\theta = 0$ ,  $z = 2$ , and  $\delta = 1$ , the inequality (4) is sharply satisfied while it is violated above four dimensions. Hence, we can conclude that in  $d > 4$  dimensions the generated cluster is no longer compact.

To deal with the question whether clusters of immune sites in systems *at* the upper critical dimension of DP,  $d_c^{\text{DP}} = 4$ , are still compact, it is worthwhile to compare the situation with a simple random walk whose upper critical dimension is  $d_c^{\text{RW}} = 2$ . The random walk is *recurrent* in  $d = 1, 2$  while it is *transient* for  $d \geq 3$  [34]. This means that the probability  $F(t)$  to visit a given site at least once until time  $t$  tends to 1 in the limit  $t \rightarrow \infty$  for  $d = 1, 2$  while it tends to a constant  $c < 1$  for  $d \geq 3$ . Therefore, the region visited by the random walker is compact in  $d \leq 2$  whereas it is not in  $d \geq 3$ . However, for  $d = 2$  the probability  $1 - F(t)$  that the site has not yet been visited decreases asymptotically as  $1 - F(t) \sim (\ln t)^{-1}$  in contrast to algebraic behavior in  $d = 1$ , where  $1 - F(t) \sim t^{-1/2}$ . This implies that in  $d = 2$  compactness is reached only slowly and we refer to this as *asymptotically* compact. Therefore, in  $d = 2$  and finite time the cluster of visited sites is highly non-compact at its boundaries and differs significantly from the one shown in Fig. 2. Using this analogy, it is near at hand to speculate that the same happens in a critical DP process. Thus, we expect the cluster of visited sites to be compact at the upper critical dimension  $d_c^{\text{DP}} = 4$  as well. However, in this case compactness should be reached considerably slower than for  $d < 4$ , i.e., we expect the clusters to be *asymptotically* compact.

The observed compactness in low dimensions leads to an important consequence regarding the critical behavior along the horizontal line in Fig. 1, as it allows the results of [27] obtained in  $d = 1$  to be generalized to 2 and 3 dimensions. In [27] the expansion of an immune region in one spatial dimension was studied in the limit of a very small probability of first infections  $p_0 \rightarrow 0$ . Using a quasi-static approximation it was shown that the survival probability does *not* obey a power law, instead it decays as a stretched exponential

$$P_s(t) \propto \exp\left(-Ap_0^{-\alpha}t^{1-\alpha}\right), \quad (6)$$



giving rise to a *finite* survival time  $T \sim p_0^{\alpha/(1-\alpha)}$ . Here  $\alpha = \nu_{\parallel}/(\nu_{\perp} + \beta_s)$  with  $\beta_s$  being the order parameter exponent next to a planar absorbing surface [35]. The main assumption made in this approximation is the compactness of the immune domain, wherefore the analysis had been restricted to  $d = 1$ . Because of the observed compactness, the same arguments can be applied in 2 and 3 dimensions so that the formula Eq. (6) should be valid in these cases as well. Inserting the known values for  $\beta_s$  [35] one obtains  $\alpha \simeq 0.947$  in  $1d$  and  $\alpha \simeq 0.72$  in  $2d$  (so far there are no estimates of  $\beta_s$  in  $3d$ ). Whether Eq. (6) is still valid at the upper critical dimension of DP,  $d_c^{\text{DP}} = 4$ , where  $\alpha$  would be  $1/2$ , is not yet clear since in this case we expect the immune region to be only asymptotically compact. The numerical verification of the stretched exponential behavior for  $d = 1$  and  $p_0 \ll p_c$  in [27] required a special enrichment method since for small  $p_0$  most simulation runs terminate after a very short time. In this paper we perform ordinary Monte Carlo simulations and therefore we do not address the numerical analysis of the horizontal line for  $p_0 \ll p_c$  in  $d > 1$ .

Another important consequence concerns the ratio of first infections and reinfections. In  $d < 4$  dimensions the average number of first infections  $n_p(t)$  (controlled by the parameter  $p_0$ ) decreases according to Eq. (3) while the average number of reinfections  $N(t)$  (controlled by the parameter  $p$ ) increases as  $t^\theta$  with  $\theta > 0$ . Thus, after sufficiently long time the parameter  $p$  controlling reinfections will have a much larger influence than the parameter  $p_0$ . As a consequence the curved phase transition line, which may be thought of as describing a situation where  $p$  and  $p_0$  balance each other, terminates in the DP point horizontally, i.e. with zero slope. In  $d \geq 4$  dimensions, primary infections and reinfections show the same scaling behavior (for  $d = 4$  probably affected by logarithmic corrections), and therefore we expect the transition line to terminate with a non-vanishing slope. We will come back to this question in Sec. 6.

#### 4. Scaling properties

The previous phenomenological arguments suggested that the behavior of the model in  $d < 4$  dimensions differs significantly from the behavior above 4 dimensions. This difference becomes also obvious when studying the corresponding Langevin equations.

According to Refs. [18, 27] the Langevin equation for the epidemic process with finite immunization reads

$$\begin{aligned} \frac{\partial}{\partial t} \rho(\mathbf{x}, t) = & a\rho(\mathbf{x}, t) - b\rho^2(\mathbf{x}, t) + D\nabla^2 \rho(\mathbf{x}, t) + \xi(\mathbf{x}, t) \\ & + \lambda \rho(\mathbf{x}, t) \exp\left(-w \int_0^t d\tau \rho(\mathbf{x}, \tau)\right), \end{aligned} \quad (7)$$

where  $\xi(\mathbf{x}, t)$  represents a density-dependent Gaussian noise with the correlations

$$\langle \xi(\mathbf{x}, t) \xi(\mathbf{x}', t') \rangle = \Gamma \rho(\mathbf{x}, t) \delta^d(\mathbf{x} - \mathbf{x}') \delta(t - t'). \quad (8)$$

It consists of the usual Langevin equation for DP plus an exponential term describing the effect of immunization. Here the exponential function can be thought of as a switch:

Initially, the integral is zero and hence the coefficient of the linear contributions in  $\rho(\mathbf{x}, t)$  is  $a + \lambda$ , representing as bare parameters the reduced rate for first infections  $p_0 - p_c$ . However, when the integrated past activity exceeds  $1/w$ , the exponential function decreases rapidly so that the additional term is essentially switched off. Roughly speaking, in a continuous description the parameter  $w$  is needed in order to specify a threshold telling us how much activity has to be accumulated at a given site in order to declare it as immune. Once the exponential term is switched off, the linear term is controlled by the coefficient  $a$  which represents the reduced reinfection rate  $p - p_c$ . In most lattice models, sites become immune after a single infection, hence the parameter  $w$  is of the order 1 while  $\lambda \sim p_0 - p$  controls the strength of immunization.

Rescaling the DP Langevin equation by

$$\mathbf{x} \rightarrow b\mathbf{x} \quad t \rightarrow b^z t \quad \rho \rightarrow b^{-\chi} \rho \quad (9)$$

with a scaling parameter  $b$  and the exponents  $z = \nu_{\parallel}/\nu_{\perp}$  and  $\chi = \beta/\nu_{\perp}$  one immediately recognizes that simple scaling invariance at the upper critical dimension  $d_c^{\text{DP}} = 4$  can only be established if  $z = \chi = 2$  and  $a = 0$ , the latter representing the critical point at the mean field level. Regarding the exponential term, scaling invariance requires the argument of the exponential function and the exponential function itself to be dimensionless, hence the coefficient  $\lambda$  and  $w$  have to be rescaled as

$$\begin{aligned} \lambda &\rightarrow b^{-y_{\lambda}} \lambda \\ w &\rightarrow b^{-y_w} w, \end{aligned} \quad (10)$$

where  $y_{\lambda} = 2$  and  $y_w = 0$ . More generally, it can be shown by a field-theoretic calculation [27] that in  $d \leq 4$  dimensions the two exponents are given by

$$y_{\lambda} = \frac{1}{\nu_{\perp}}, \quad y_w = \frac{\nu_{\parallel} - \beta}{\nu_{\perp}}. \quad (11)$$

As  $y_w$  and  $y_{\lambda}$  are positive, the exponential term for immunization is relevant in  $d \leq 4$  dimensions. Expanding the exponential function as a Taylor series, the resulting terms would be equally relevant in  $d = 4$  and *increasingly relevant* in  $d < 4$  dimensions. Therefore, in  $d \leq 4$  dimensions a Taylor expansion of the exponential function in Eq. (7) is meaningless in the renormalization group sense, instead it has to be kept in as a whole. This circumstance is probably responsible for the observed non-universality along the horizontal line in Fig. 1.

In  $d > 4$  dimensions, however, the situation is different. Here, power counting at the upper critical dimension of DyP,  $d_c^{\text{DyP}} = 6$ , yields  $y_w < 0$ , meaning that the relevancy of the terms in the Taylor expansion decreases. In this case it is legitimate to carry out the Taylor expansion, keeping only the most relevant contribution. As the zeroth order can always be absorbed in a redefinition of  $a$ , the most relevant contribution is the first-order term  $-\lambda w \rho(\mathbf{x}, t) \int_0^t d\tau \rho(\mathbf{x}, \tau)$ . In addition we may drop the quadratic contribution  $-b\rho^2(\mathbf{x}, t)$ , which is irrelevant at  $d_c^{\text{DyP}} = 6$ , leading to the Langevin equation

$$\frac{\partial}{\partial t} \rho(\mathbf{x}, t) = (a + \lambda) \rho(\mathbf{x}, t) + D \nabla^2 \rho(\mathbf{x}, t) + \xi(\mathbf{x}, t) \quad (12)$$

$$- \lambda w \rho(\mathbf{x}, t) \int_0^t d\tau \rho(\mathbf{x}, \tau).$$

corresponding to the field theory studied in [16, 18]. In contrast to Eq. (7) the influence of immunization is effectively described by a single parameter, namely, by the product  $\lambda w$ . Assuming  $y_w$  to be negative for any  $d > 4$  this scenario is expected to hold even in presence of fluctuation effects. Moreover, in contrast to Eq. (7) the parameter now appears in the prefactor of the linear term, shifting the parameter  $a$ . This suggests, in accordance with the preceding section, that at least in  $4 < d \leq 6$  dimensions the reduced first infection and reinfection probability (here corresponding to  $\lambda$  and  $a$ ) scale identically and that the phase transition line, along which the influence of  $a$  and  $\lambda$  is balanced, terminates with a nonzero slope in the DP point.

To summarize we arrive at the following picture:

- In  $d \leq 4$  dimensions the EPFI is described by Eq. (7), in which an expansion of the exponential function is not allowed. The exponential function is conjectured to produce non-universal features such as a stretched exponential decay of the survival probability, as observed in  $d = 1$  dimensions [27].
- In  $4 < d \leq 6$  the process is described by Eq. (12). Fluctuation effects are still present and the corresponding field theory is well-defined and renormalizable [18].
- In  $d > 6$  the mean field approximation becomes valid. The system is driven to a trivial Gaussian fixed point, which is the same for GEP and DP.

## 5. Phase Diagrams

Fig. 4 presents phase diagrams of the epidemic process with finite immunization for spatial dimensions  $d = 3, 4, 5, 6$  which were obtained from MC simulations (see Sec. 2). The horizontal lines obey  $p = p_c$  with the values of  $p_c$  given in Tab. B1. The lines connecting the DP and the GEP point were determined as follows. First we performed spreading simulations at the critical point of the GEP, i.e., for  $p = 0$ , using the critical values of bond percolation given in [30]. Thereby, we estimated various critical exponents for DyP which are presented in Tab. C1. In order to locate the phase transition line, we then used the fact that the critical behavior along this line is that of dynamical percolation. We determined various critical points along the lines by keeping  $p$  fixed and varying  $p_0$  until the quantities  $P_s(t)$ ,  $N(t)$  and  $R^2(t)$ , see Eq. (1), displayed the expected slope corresponding to DyP in a log-log plot.

In accordance with the predictions of Sec. 3 the data indeed suggests that the curved phase transition line terminates at the DP point with vanishing slope for  $d = 3$  and with finite slope for  $d \geq 4$ . For  $d = 4$  this behavior is not so clear cut and we believe that this is caused by logarithmic corrections at the DP point.

Assuming that the curved phase transition line behaves in the vicinity of the DP point as  $p_{0,c}(p) - p_c \sim (p_c - p)^\gamma$ , our data leads to  $\gamma = 0.47(7)$  for  $d = 2$  and to

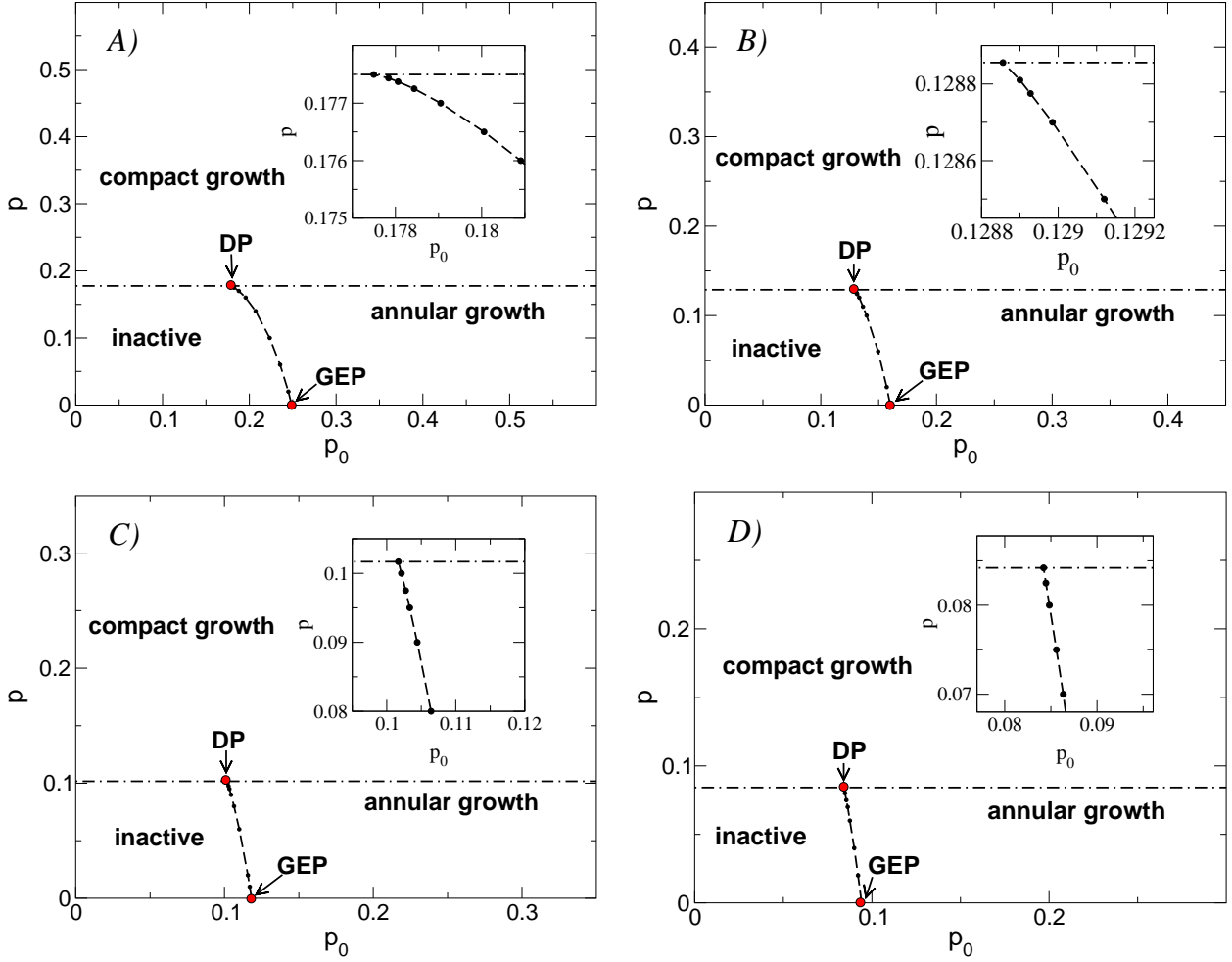


**Figure 4.** Phase diagrams for the EPFI for  $d = 3, 4, 5, 6$ , A)–D), determined from MC simulations. The insets show the vicinity of the DP point. Circles mark the numerically determined critical points.

$\gamma = 0.74(8)$  for  $d = 3$ . Since the error bars are rather large, our data does only allow a rough estimate of  $\gamma$  and we did not further attempt to relate its value to other critical exponents.

## 6. Temporal correlation length in the vicinity of the DP point

Off criticality but in the vicinity of the DP point, i.e.,  $p = p_c \pm \tilde{\epsilon}$ ,  $p_0 = p_c \pm \epsilon$ , one initially observes the critical behavior of DP until the process eventually crosses over to a different type of behavior. This crossover takes place at a certain typical time scale  $\xi_{\parallel}$ . If  $\tilde{\epsilon} \neq 0$  (moving vertically away from the DP point) one expects that asymptotically  $\xi_{\parallel} \sim \tilde{\epsilon}^{-\nu_{\parallel}}$  with the critical DP exponent  $\nu_{\parallel}$  for the temporal correlation length. The reason is the following. Near the DP point, for  $d < 4$ , the process is dominated by reinfections that perform an ordinary DP process with parameter  $p$  on a compact region (see Sec. 3). It is only on the edge of the visited region where the first infection probability  $p_0$  plays a role.

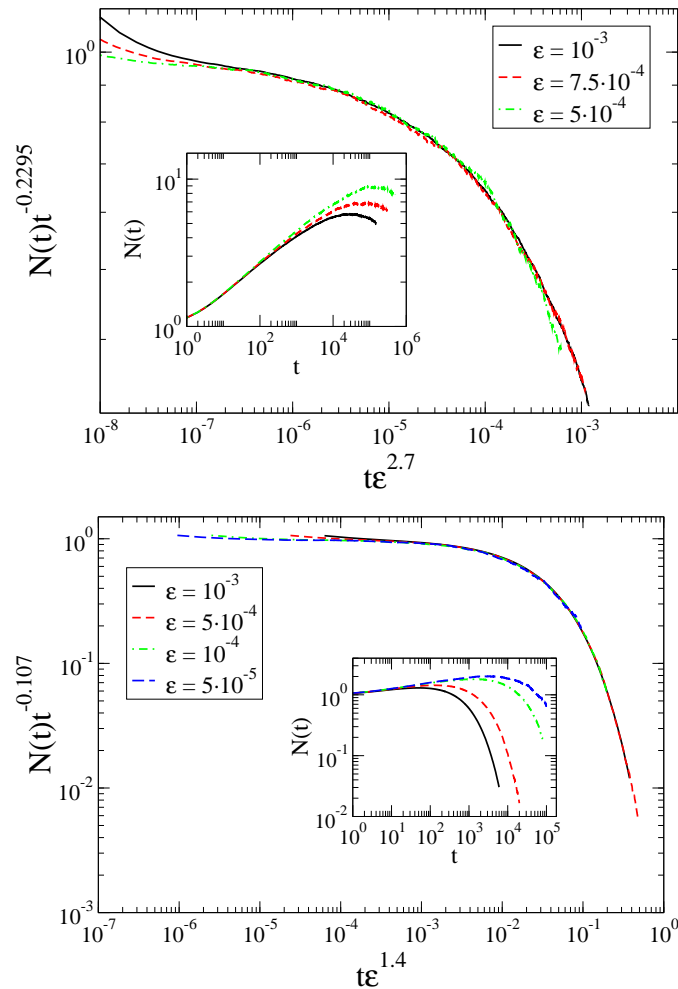


**Figure 5.** Data collapses for  $p = p_c$  and  $p_0 = p_c - \epsilon$  for  $d = 2$  (top) and  $d = 3$  (bottom).  $N(t)$  is scaled with  $t^\theta$  with the values of  $\theta$  from Tab. B1. The time is scaled with  $\epsilon^\mu$  such that the best data collapses were obtained. The insets show the original data.

Hence, the time scale associated with  $\tilde{\epsilon}$  is expected to be smaller than that associated with a change  $\epsilon$  of  $p_0$ . For  $d \geq 4$ , primary infections and reinfection show equal scaling behavior and therefore one expects both times to scale in the same way.

We are left with the question how the temporal correlation length behaves for  $p = p_c$  and  $p_0 = p_c \pm \epsilon$  (moving horizontally away from the DP point) in  $d < 4$ . Although we expect non-universal behavior on the horizontal line it may nevertheless be possible to identify an exponent  $\mu$  for the temporal correlation length

$$\xi_{\parallel} \sim \epsilon^{-\mu} \quad (13)$$

in the vicinity of the DP point,  $\epsilon \ll 1$ . In fact, as shown in Fig. 5, plotting  $N(t)t^{-\theta}$  versus  $t/\xi_{\parallel}$  we can produce a data collapse by tuning  $\mu$ . With similar simulations in

$d = 4, 5$  (not shown here) we get the estimates

$$\mu = \begin{cases} 2.7(7) & \text{in } d = 2 \\ 1.4(2) & \text{in } d = 3 \\ 1.1(13) & \text{in } d = 4 \\ 1.0(1) & \text{in } d = 5 \end{cases} \quad (14)$$

Obviously, in  $d < 4$  the exponent  $\mu$  differs from  $\nu_{\parallel}$  ( $\nu_{\parallel} = 1.295$  for  $d = 2$  [36] and  $\nu_{\parallel} = 1.105$  [37] for  $d = 3$ ). Because of logarithmic corrections, it is likely that  $\mu = 1$  in  $d = 4$  as well. With decreasing dimension the value of  $\mu$  and therewith the simulation time increases rapidly. For this reason the estimate for  $d = 2$  is less precise, while simulations in  $d = 1$  turned out to be unreliable. However, for  $d = 3$  the data collapse is fairly good. In App. Appendix A we present a heuristic argument for the value of  $\mu$  in accordance with the numerical data.

## 7. Summary

We studied a model for spreading with finite immunization which is controlled by probabilities for first infections ( $p_0$ ) and reinfections ( $p$ ). We focussed in particular on the critical behavior close to the directed percolation point, especially in high dimensions  $d > 2$ . We argued that we expect the domains of immune sites to be compact for  $d \leq 4$ , however, with an approach to compactness that is (logarithmically) slow at the upper critical dimension of DP,  $d_c^{\text{DP}} = 4$ . Therefore, we denoted the visited region as asymptotically compact in  $d = 4$ . The compactness of the immune region was supported by MC-simulations. We pointed out that this compactness implies that a recently introduced scaling argument, suggesting a stretched exponential decay of the survival probability for  $p = p_c$ ,  $p_0 \ll p_c$  in one spatial dimension, should apply in any dimension  $d \leq 3$  and maybe in  $d = 4$  as well. Furthermore, we showed that for  $d < 4$  the number of first infections (averaged over all runs) decreases whereas the number of reinfections increases. Contrarily, for  $d \geq 4$  both quantities scale equally. From that we derived the result that the phase transition line connecting the GEP and the DP point terminates in the DP point with a *finite* slope for  $d \geq 4$  and with a vanishing slope for  $d < 4$ , which was supported by numerically determined phase diagrams. We also discussed the Langevin equation for the process, in order to study how the properties of the process change depending on the spatial dimension. Investigating the behavior for  $p = p_c$  and  $p_0 = p_c - \epsilon$ ,  $\epsilon \ll 1$  we were able to identify an exponent  $\mu$  for the temporal correlation length which is different from  $\nu_{\parallel}$  for DP.

### Acknowledgments:

Parts of the numerical simulations were carried out on the 128-node Alpha Linux Cluster Engine ALICE at the University of Wuppertal. We thank N. Eicker, T. Lippert, and B. Orth for technical support. Moreover, we are grateful to two referees for bringing references [40, 42, 43] to our attention.

## Appendix A. Speculation about the value of $\mu$

In the following we present a heuristic argument for the value of  $\mu$  in  $d \leq 4$  dimensions that is in accordance with the numerical results presented above. Consider first a subcritical DP process governed by the parameter  $p = p_c - \epsilon$ ,  $\epsilon \ll 1$ . Initially the system behaves as if it was critical until the hostile conditions eventually lead to extinction. This happens on a time scale  $\xi_{\parallel} \sim \epsilon^{-\nu_{\parallel}}$ . During the active time the process produces active sites according to  $N(t) \sim t^{\theta}$ , see Eq. (1). Therefore, a subcritical DP process activates on the whole  $M$  sites before it dies out, where  $M$  scales as  $M \sim \epsilon^{-\nu_{\parallel}(\theta+1)}$ . Consider now the EPFI with  $p = p_c$  and  $p_0 = p_c - \epsilon$  which dies out on a time scale  $\xi_{\parallel} \sim \epsilon^{-\mu}$ . In this case (for  $d \leq 4$ ) one has basically a critical DP process in the compact interior region of the immune cluster and a subcritical process on its edge. The integrated activity on the edge scales as  $I(t) \sim t^{d/z-\delta}$ , see Eq. (2). If one assumes that the critical reinfections do not introduce a time scale and that the process on the edge is subject to the same bound as subcritical DP concerning the maximal activity, one arrives at  $I \sim M$  leading to

$$\mu = \frac{z\nu_{\parallel}(\theta + 1)}{d - \delta z}. \quad (\text{A.1})$$

With the critical exponents of DP given in Sec. 6 and in Tab. B1 Eq. (A.1) results in  $\mu \approx 2.335$  for  $d = 2$ ,  $\mu = 1.437$  for  $d = 3$  and  $\mu = 1$  for  $d = 4$  which is compatible with the numerical results. For  $d = 1$ , with Tab. B1 and  $\nu_{\parallel} = 1.7338$  [38] one obtains  $\mu \approx 4.814$ . However, this argument needs to be substantiated and therefore Eq. (A.1) has to be taken with care.

## Appendix B. DP in high dimensions

In this Appendix we report some numerical results on directed bond percolation in high dimensions. The values are partly more precise than previously reported estimates. Similar results for directed site percolation in  $d = 3, 4$ , and 5 dimensions were recently reported in [25, 32].

Table B1 shows the results for directed bond percolation ranging from 1 to 7 spatial dimensions. Our estimates for  $d = 3$  differ slightly from that presented previously by Dickman [40], namely,  $\delta = 0.7263(11)$ ,  $\theta = 0.110(1)$  and  $z = 1.919(4)$ . Though the error bars in [40] are smaller than in our case, our data is incompatible with the values of  $\delta$  and  $z$  in [40]. We do not conclude with respect to this issue but note that further numerical effort in this context is desirable. The value  $\theta = 0.107(5)$  is smaller than Dickmans result  $\theta = 0.110(1)$  but larger than the field-theoretic estimate  $\theta = 0.098$  [41] based on a two-loop calculation.

Finally we note that our estimates in  $3d$  are compatible with the DP hyperscaling relation [28, 33] where, inserting our estimates for  $z$  and  $\delta$ , we obtain

$$\theta = d/z - 2\delta = 0.107(10) \quad (\text{B.1})$$

$d$	$p_c$	$\delta$	$\theta$	$z$	Ref.
1	0.644700185(5)	0.159464(6)	0.313686(8)	1.580745(10)	[38]
2	0.287338(3) <sup>†</sup>	0.4505(10)	0.2295(10)	1.766(2)	[36]
3	0.1774970(5)	0.737(5)	0.107(5)	1.897(5)	present work
4	0.1288557(5)	1*	0*	2*	present work
5	0.1016796(5)	1	0	2	present work
6	0.0841997(14)	1	0	2	present work
7	0.07195(5)	1	0	2	present work

**Table B1.** Numerical results for directed bond percolation on a simple  $d$ -dimensional cubic lattice. For  $d = 4$ , \* denotes that the mean-field behavior is subjected to logarithmic corrections.  $z = \nu_{\parallel}/\nu_{\perp}$ . <sup>†</sup> Taken from [39].

$d$	$p_c$	$\delta$	$\theta$	$z$	Ref.
2	0.5 <sup>†</sup>	0.092	0.586	1.1295	[44] <sup>‡</sup>
3	0.2488125(25)	0.346(6)	0.488(7)	1.375(5)	present work
4	0.1601310(10)	0.595(8)	0.30(1)	1.605(9)	present work
5	0.1181718(3)	0.806(12)	0.134(10)	1.815(10)	present work
6	0.0942019(6)	1*	0*	2*	[30]

**Table C1.** Numerical results for dynamical bond percolation on a simple  $d$ -dimensional cubic lattice. For  $d = 6$ , \* denotes that the mean-field behavior is subjected to logarithmic corrections.  $z = \nu_{\parallel}/\nu_{\perp}$ . <sup>†</sup> Taken from [15]. <sup>‡</sup> Uncertainties are in the last digit. For  $d = 1$  the transition is shifted to  $p_c = 1$ .

In  $d > 4$ , however, the hyperscaling relation is violated.

### Appendix C. Dynamical percolation in high dimensions

Here we present our numerical estimates for the values of critical thresholds and exponents for dynamical bond percolation on a  $d$ -dimensional cubic lattice. Note that, as far as we know, no numerical values for critical exponents for DyP in  $d = 4, 5$  have been published before. The values presented for  $d = 3$  are compatible with precise estimates published previously, i.e.,  $p_c = 0.2488126(5)$  [42],  $\delta = 0.345(4)$ ,  $\theta = 0.494(6)$  and  $1/z = 0.728(2)$  where the latter values are from [43].

The value of  $\theta = 0.488(7)$  is incompatible with the value of  $\theta = 0.536$  reported in [44] based on previous estimates from [45]. However, in this case  $\theta$  was not directly measured but obtained via scaling relations, which presumably is the reason for the considerable difference between the two estimates.

The estimates given in Tab. C1 are compatible with the hyperscaling relation for DyP [33, 43]. For  $d = 3, 4, 5$  we obtain

$$\theta = d/z - 2\delta - 1 = \begin{cases} 0.49(2) & \text{for } d = 3, \\ 0.30(3) & \text{for } d = 4, \\ 0.14(4) & \text{for } d = 5. \end{cases} \quad (\text{C.1})$$



## References

- [1] Marro J and Dickman R, *Nonequilibrium phase transitions in lattice models*, Cambridge University Press, Cambridge (1999).
- [2] Hinrichsen H, *Non-equilibrium critical phenomena and phase transitions into absorbing states*, 2000 Adv. Phys. **49**, 815 [cond-mat/0001070].
- [3] Ódor G, *Universality classes in nonequilibrium lattice systems*, submitted [cond-mat/0205644v7].
- [4] Hinrichsen H, *On possible experimental realizations of Directed Percolation*, 2000 Braz. J. Phys. **30**, 69 [cond-mat/9910284].
- [5] Mollison D, *Spatial contact models for ecological and epidemic spread*, 1977 J. R. Stat. Soc. B **39**, 283.
- [6] Dammer S M and Hinrichsen H, *Epidemic spreading with immunization and mutations*, 2003 Phys. Rev. E **68**, 016114 [cond-mat/0303467].
- [7] Ziff R M, Gulari E, and Barshad Y, *Kinetic phase-transitions in an irreversible surface-reaction model*, 1986 Phys. Rev. Lett. **56**, 2553.
- [8] Hinrichsen H, Jiménez-Dalmaroni A, Rozov Y, and Domany E, *Flowing sand - a physical realization of Directed Percolation*, 1999 Phys. Rev. Lett. **83**, 4999 [cond-mat/9908103].
- [9] Hinrichsen H, Jiménez-Dalmaroni A, Rozov Y, and Domany E, *Flowing sand - a possible physical realization of Directed Percolation*, 2000 J. Stat. Phys. **98**, 1149 [cond-mat/9909376].
- [10] Kinzel W, *Phase transitions of cellular automata*, 1985 Z. Phys. B **58**, 229.
- [11] Moshe M, *Recent developments in Reggeon field theory*, 1978 Phys. Rep. C **37**, 255.
- [12] Grassberger P and Sundermeyer K, *Reggeon field theory and Markov processes*, 1978 Phys. Lett. B **77**, 220.
- [13] Cardy J L and Sugar R L, *Directed percolation and Reggeon field theory*, 1980 J. Phys. A **13**, L423.
- [14] Grassberger P, *On the critical behavior of the general epidemic process and dynamical percolation*, 1983 Math. Biosci. **63**, 157.
- [15] Stauffer D and Aharony A, *Introduction to Percolation Theory*, 2nd ed., Taylor & Francis, London (1992).
- [16] Cardy J L and Grassberger P, *Epidemic models and percolation*, 1985 J. Phys. A **18**, L267.
- [17] Grassberger P, Chaté H, and Rousseau G, *Spreading in media with long-time memory*, 1997 Phys. Rev. E **55**, 2488.
- [18] Janssen H K, *Renormalized field theory of dynamical percolation*, 1985 Z. Phys. B **58**, 311.
- [19] Janssen H K, Müller M, and Stenull O, *A Generalized Epidemic Process and Tricritical Dynamic Percolation*, submitted [cond-mat/0404167].
- [20] Jensen I, *Critical behavior of the pair contact process*, 1993 Phys. Rev. Lett. **70**, 1465.
- [21] Jensen I and Dickman R, *Nonequilibrium phase transitions in systems with infinitely many absorbing states*, 1993 Phys. Rev. E **48**, 1710.
- [22] Muñoz M A, Grinstein G, Dickman R, and Livi R, *Critical behavior of systems with many absorbing states*, 1996 Phys. Rev. Lett. **76**, 451.
- [23] Muñoz M A, Grinstein G, and Dickman R, *Phase structure of systems with infinite numbers of absorbing states*, 1998 J. Stat. Phys. **91**, 541.
- [24] F. van Wijland, *Universality class of nonequilibrium phase transitions with infinitely many absorbing states*, 2002 Phys. Rev. Lett. **89**, 190602.
- [25] Lübeck S and Willmann R D, *Universal scaling behaviour of directed percolation and the pair contact process in an external field*, 2002 J. Phys. A **35**, 10205.
- [26] López C and Muñoz M A, *Numerical analysis of a Langevin equation for systems with infinite absorbing states*, 1997 Phys. Rev. E **56**, 4864.
- [27] Jiménez-Dalmaroni A and Hinrichsen H, *Epidemic processes with immunization*, 2003 Phys. Rev. E **68**, 036103 [cond-mat/0304113].
- [28] Grassberger P and de la Torre A, *Reggeon field theory (Schlögl's first model) on a lattice - Monte-Carlo calculations of critical behavior*, 1979 Ann. Phys. **122**, 373.

- [29] Janssen H K, *Survival and Percolation Probabilities in the Field Theory of Growth Models*, submitted [cond-mat/0304631].
- [30] Grassberger P, *Critical percolation in high dimensions*, 2003 Phys. Rev. E **67**, 036101.
- [31] Janssen H K and Stenull O, *Logarithmic Corrections in Directed Percolation*, 2004 Phys. Rev. E **69**, 016125.
- [32] Lübeck S and Willmann R D, *Universal scaling behavior of directed percolation around the upper critical dimension*, 2004 J. Stat. Phys **115**, 1231 [cond-mat/0401395].
- [33] Muñoz M A, Grinstein G and Tu Y, *Survival probability and field theory in systems with absorbing states*, 1997 Phys. Rev. E **56**, 5101.
- [34] Spitzer F, *Principles of Random Walk*, Springer-Verlag, New York, second-edition, (1976).
- [35] Fröjdh P, Howard M, and Lauritsen K B, *Directed percolation and other systems with absorbing states: Impact of boundaries*, 2001 Int. J. Mod. Phys. **15**, 1761, and references therein.
- [36] Voigt C A, Ziff R M, *Epidemic analysis of the second-order transition in the Ziff-Gulari-Barshad surface-reaction model*, 1997 Phys. Rev. E **56**, R6241.
- [37] Jensen I, *Critical behavior of the 3-dimensional contact process*, 1992 Phys. Rev. A **45**, R563.
- [38] Jensen I, *Low-density series expansions for directed percolation: I. A new efficient algorithm with applications to the square lattice*, 1999 J. Phys. A **32**, 5233.
- [39] Grassberger P and Zhang Y C, *"Self-organized" formulation of standard percolation phenomena*, 1996 Physica A **224**, 169.
- [40] Dickman R, *Reweighting in nonequilibrium simulations*, 1999 Phys. Rev. E **60**, R2441.
- [41] Janssen H K, *On the non-equilibrium phase transition in reaction-diffusion systems with an absorbing stationary state*, 1981 Z. Phys. B **42**, 151.
- [42] Lorenz C D and Ziff R M, *Precise determination of the bond percolation thresholds and finite-size scaling corrections for the sc, fcc, and bcc lattices*, 1998 Phys. Rev. E **57**, 230.
- [43] Grassberger P, *Numerical studies of critical percolation in three dimensions*, 1992 J. Phys. A **25**, 5867.
- [44] Muñoz M A, Dickman R, Vespignani A and Zapperi S, *Avalanche and spreading exponents in systems with absorbing states*, 1999 Phys. Rev. E **59**, 6175.
- [45] Bunde A and Havlin S, in *Fractals and Disordered Systems*, ed. by Bunde A and Havlin S, Springer-Verlag, Heidelberg, (1991).